Proceedings of the 17th World Congress
The International Federation of Automatic Control
Seoul, Korea, July 6-11, 2008

Development of a Foot Mechanism for Landing Experiment

Seyoung Cheon *,**, **Yonghwan Oh** *, **Younghwan Chang** *, **Youngpil Park** **

* *Center for Cognitive Robotics Research, Korea Institute of Science and Technology, Seoul, 136-791, Republic of Korea (Fax:+82-2-9585749; e-mail : cheon798 , oyh @ kist.re.kr)*
** *Department of Electrical & Electronic Engineering Department, Yonsei University, Seoul, Korea, (e-mail: mignpark@yonsei.ac.kr)*

Abstract:
For the stable landing of a humanoid walking, a humanoid foot needs to reduce an impact from the ground reaction force and does not cause ZMP variation when its foot is landing. To satisfy the above condition, this paper introduces the newly designed foot mechanism has an additional shock absorbing material and guided equipment which constrains translational direction. The ability of the proposed foot mechanism is shown as the experiment which is performed in landing leg platform. The landing leg platform provides the same landing effect and a variety of condition that a humanoid robot may be faced with various environments when the humanoid foot is landing. The two kinds of experiments are performed. One verifies the capability of additional shock absorbing material and the other shows the effect of the guided equipment.

1. INTRODUCTION

Recently, the study of a biped robot that has a high mobility compared with a mobile robot in narrow space is active. The stable walking should be guaranteed in order to procure a high mobility. For the stable walking, it is important to research the end-effector which interacts with an environment. During the biped robot walking, the ground reaction force influences the stability. The humanoid foot mechanism should have a passive compliant material which decreases landing impact force to protect the force-torque sensor and robot itself in vertical direction (S. Kajita et al., 2001). And to prevent the vibration of leg compliance control, the humanoid has rubber bushes inserted into a guide in its feet. It deforms elastically in the vertical direction upon a force being transmitted from the sole (K. Hirai et al., 1998).

The foot does not have particular equipment except for a sole and a sole material (I. W. Park et al., 2005). In case of this foot, the landing impact force is absorbed only with sole material mechanically. Also, a passive compliant material or a rubber bush induces additionally translational force which causes ZMP variation. A proposed foot in this paper has two kinds of materials which can absorb the landing impact force. One is the sole material which is attached at the sole and the other is the all directional rubber bush. And to inhibit ZMP variation, the proposed foot has a guide equipment which is consist of a linear guide and a guide shaft, a guide stopper. This paper introduces a newly designed foot mechanism and shows whether the proposed foot is suitable in humanoid foot. The newly designed foot mechanism satisfies above two functions. The experiment about the foot mechanism is performed and verified on the lading leg platform. For convenience, we call the rigid foot which has only sole and sole material.

Hence, this paper addresses as follows: Section 2 describes the mechanical specification of the landing leg platform and a brief introduction of algorithm that based on CLIK of the landing leg. The newly designed foot mechanism is mentioned in section 3 with its design concept and the experiment about the shock absorbing material is performed. In section 4, the experiment about ZMP variation is performed and the result is shown.

Fig. 1. Newly designed foot and landing leg platform

2. LANDING LEG PLATFORM

A landing leg platform could provide landing motion repeatedly which provides the same effect of humanoid robot landing during walking.

2.1 Mechanical Design and Specification of Landing Leg Platform

A landing leg platform has four degrees of freedom (DOF). A hip pitch and knee pitch joint has one DOF respectively. An ankle pitch and roll joint has one DOF respectively. The system has two linear guides, two guide shafts and four stoppers which provide the same effect as a supporting leg does. The landing plate can adjust an inclination of a landing area with a block that has a slope. It is shown in Fig.2.

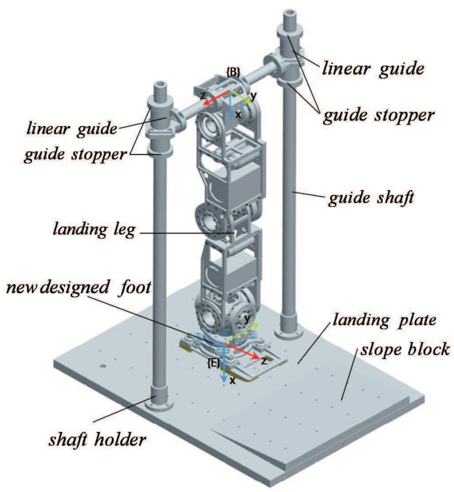

Fig. 2. Mechanical design of landing leg platform

2.2 System Integration

We used a Xenomai 2. 2. 2 with Linux Kernel ver. 2. 6. 17 on Fedora Core ♯ 5 to guarantee real.time control. This software allows us to make the control thread with the highest priority so that user can control the system in real-time. In real time operating system(RTOS : Linux with Xenomai 2. 2. 2), a communication between user mode and kernel mode used a pipe line. The high level system(Operating System : Xenomai 2. 2. 2) sends the reference data which are motor position and velocity data to the DSP controller (the low level system) at an interval of 5ms(200Hz), then the DSP controller interpolates linearly the reference position and velocity data at an interval of 1ms(1 KHZ) and makes PWM signal sending to a motor driver board. For the communication bus line, the IEEE1394 protocol was established between the main real time operating system and the sub-controller (B. J. You et al., 2005). A 6-axis force torque sensor sends a force torque data at an interval of 0.125ms(8 KHz). But we use the data sampled 200Hz. The bus line and force torque sensor line uses each an exclusive cable and a PCI card respectively.

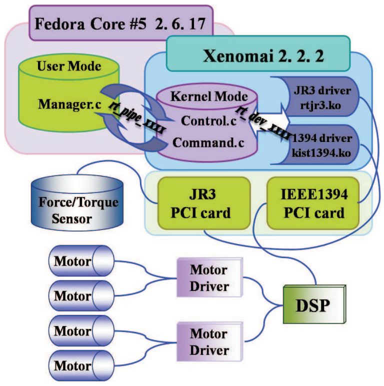

Fig. 3. Control architecture of landing leg platform system

2.3 Inverse Kinematics Algorithm

The landing motion is made up of a motion trajectory which consists of several point to point motions with time sections. The point to point motion trajectory is presented with utilizing the quintic polynomial. The orientation of the actual posture vector can be specified in terms of minimal representation (Fixed ZYX Euler angles). The roll angle is .90 respectively because of system configuration. The actual posture vector which shows position and orientation of the end-effector frame with respect to the base frame is computed using the equation (1) (L. Sciavicco et al., 1996).

$$x_{act}(t_k) = k(q_{act}(t_{act})) \tag{1}$$

And the error which subtracts the actual posture from the posture of trajectory is defined as follows.

$$e(t_k) = x_{dsg}(t_k) - x_{act}(t_k) \tag{2}$$

$$\dot{e}(t_k) = \dot{x}_{dsg}(t_k) - J_A(q_{act})\dot{q}_{act} \tag{3}$$

The choice of the relationship between $q_{act}(t_k)$ and $e(t_k)$ allows finding inverse kinematics algorithm with different performance.

$$\dot{q}_{des}(t_k) = {J_A^{\dagger}}^{-1}(q_{act}(t_k))(\dot{x}_{dsg}(t_k) + Ke(t_k)) \tag{4}$$

$$q_{des}(t_k) = q_{act}(t_k) + \dot{q}_{act}(t_k)\Delta t \tag{5}$$

where K is a positive definite matrix and the system is asymptotically stable. The error tends to be zero along the trajectory with a convergence rate that depends on the eigenvalues of matrix K (L. Sciavicco et al., 1996). And $J_A^{\dagger}$. is pseudo inverse because that the system has four DOF. The above two equations give a desired joint

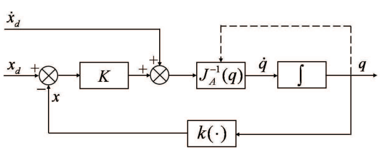

Fig. 4. Block diagram of the inverse kinematics algorithm

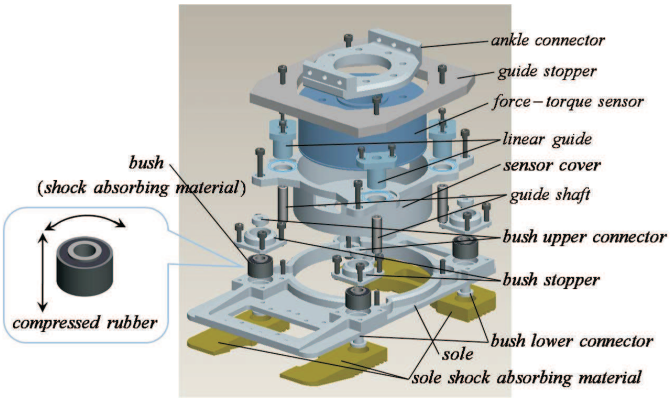

Fig. 5. Deal drawing of the proposed foot mechanism

position and velocity at a certain time so that the end-effector frame follows the desired trajectory. A total block diagram is shown in Fig. 4.

3. SHOCK ABSORBING PERFORMANCE

A landing impact force is just absorbed by a sole material because that rigid foot of a humanoid consists of sole and sole material. Only a sole material is insufficient to absorb a landing impact force. Though a sole material is a flexible material which is enough to reduce impact force, this material is not in role of the sole material because that a flexible material induces translational force which makes ZMP variation and this variation deteriorates the stability of humanoid. Therefore, the humanoid foot has the sole material that has not influence on the ZMP variation and the sole material has a sufficient shock absorbing effect at the same time. However it is not easy to find a material which satisfies above conditions. This paper introduces the newly developed foot mechanism which can not only reduced impact force but also inhibit the induced force which is a cause of ZMP variation by sole material.

3.1 Newly developed foot mechanism

The proposed foot has an additional shock material, called a bush besides the sole material. It is shown in Fig. 5. So, the sole material has not need to be a soft material that induces ZMP variation. The bush connected the sole with the sensor cover provides the flexibility which operates to all directions between the two parts. This flexibility provided by the bush protects the force-torque sensor and the robot itself from the landing impact force. However the bush induces the lateral movement. This movement is a cause of a ZMP variation. To prohibit this movement, the propose foot has four linear guides and guides shaft, one guide stopper. The shock absorbing performance that appears with adding the bush is shown in following sub-section. The effect of guide equipment is shown in the next section.

3.2 Process of the landing experiment

The process of the landing experiment consists of five phases as shown in Fig. 6. In the phase, called raisingfoot, the foot is raised 0.04m from the landing plate. And then the foot lands on 0.001m below on the plate. That makes

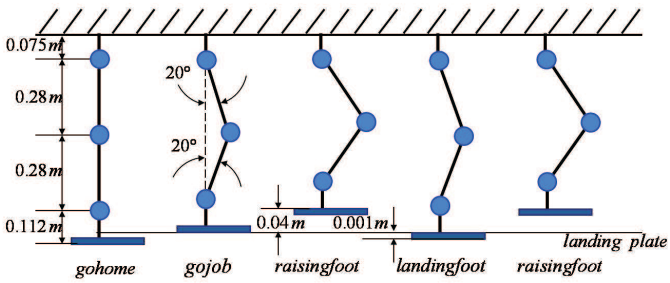

Fig. 6. Process of landing experiment

more vertical force than the phase, called gojob. The landing is fulfilled for 0.75 sec. Then the foot maintains the previous posture for 2.5 sec and is raised.

3.3 Result of the experiment

Selected sole materials in the shock absorbing experiment are a urethane pad, a fluoro rubber sheet, a butyl rubber sheet and a silicon pad. The first landing experiment is about previous foot with only sole material. The urethane pad shows the highest peak. The next is a fluoro rubber sheet. Both a butyle rubber sheet and a silicon pad have a similar impact peak. The result is shown in Fig. 7.

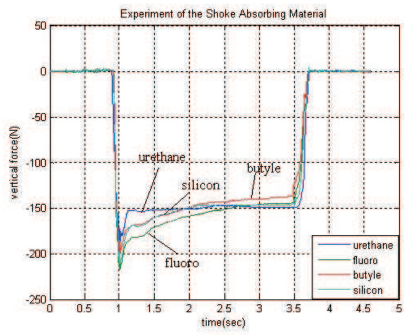

Fig. 7. Result of a shock absorbing performance for each material

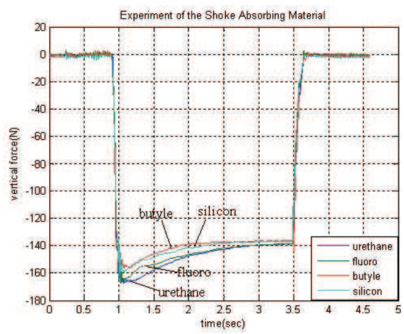

Fig. 8. Result of a shock absorbing performance with bush

Fig. 8 shows the result of the proposed foot with bush. The result presents that the bush could absorb the impact force more than the foot with sole material only. And the total shapes are similar with each material irrespective of sole material. So to speak, the characteristic of a bush gets rid of the effects of sole materials. Fig. 9 shows comparison between foots which select a fluoro rubber sheet to sole material.

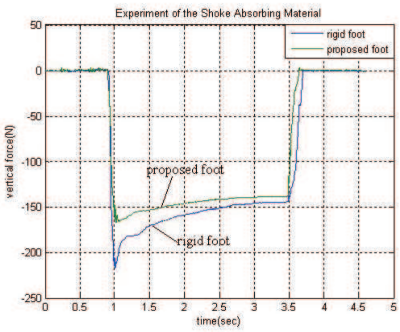

Fig. 9. Comparison between the rigid foot and the proposed foot with a fluoro rubber sole material

4. EFFECT OF GUIDE EQUIPMENT

In the previous section, the bush can absorb the shock when the foot lands on the plate. Namely, the proposed foot mechanism decreases the vertical impact of the ground reaction force. However, because the bush can move all direction, it induces additionally translational force. These forces cause ZMP variation.

4.1 Guide equipment

In this paper, a linear guide and guide stopper are proposed. A linear guide makes the sensor part (sensor cover shown in Fig. 5) move only up and down. A linear guide has ball bearings in its inside, and guide shaft does a vertical movement among the bearings. But, as all mechanical products like bearings have a tolerance, the linear guide has a minute tolerance. These cause translational movement and lateral force. To compensate this, the proposed foot is equipped with a guide stopper. The guide stopper is fixed at guide shaft with a minute gap from the upper side of the linear guide.

4.2 Excitation experiment

To show the effect of the guide equipment of the proposed foot mechanism, the excitation experiment is performed. The landing leg is equipped with three kinds of foot. One is the previous rigid foot and another is the proposed foot with only bush, the other is the proposed foot with bush and guide equipment. A sole material is removed from all foots to only analyze the characteristic of bush and guide equipment. To analyze and compare, a single mass inverted pendulum with compliant joint is considered as a simple model as shown in Fig. 10.

$$mgl\theta_{act} - ml^2\ddot{\theta}_{act} = \tau_{act} \tag{6}$$

$$\tau_{act} = \tau_{des} + K(\theta_{des} - \theta_{act}) \tag{7}$$

where θ_{des} denotes the desired ankle joint and θ_{act} denotes the actual inclined angle produced by the compliance. K_{leg} and K_{foot} are the stiffness of a leg and a foot, respectively. we assume that the each stiffness is connected by serial.

So, the stiffness is this: $\frac{1}{K} = \frac{1}{K_{foot}} + \frac{1}{K_{leg}}$. m is a concentrated mass of the system and l is the length of the

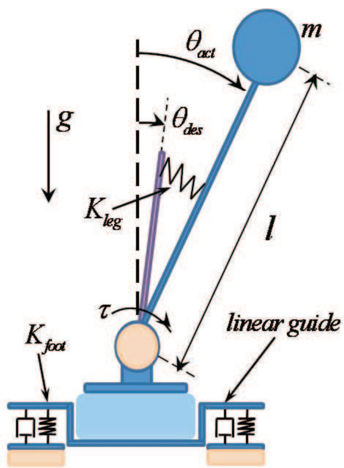

Fig. 10. Simple inverted pendulum model

massless bar which connects the concentrated mass with the joint. And the damping coefficient is neglected in this paper, since its value is relatively small compared to the stiffness.

The effect of bush with the guide equipment is contained and shown to the total stiffness of landing leg. The previous foot has the highest stiffness and resonance frequency. And the proposed foot which is shown in Fig. 5 has the more small stiffness and resonance than the previous rigid foot, because of a minute tolerance which exists between mechanical structures. Finally the proposed foot without the guide equipment has the lowest stiffness and resonance frequency. The total stiffness and natural frequency are obtained by followed equations.

$$\omega_n = \sqrt{\frac{g}{l}} \tag{8}$$

$$K = \frac{\tau_{act} - \tau_{des}}{\theta_{err}} \tag{9}$$

where $\theta_{err}(= \theta_{des} - \theta_{act})$ denotes the error of the joint value. The center of mass which is called CoM of the system is [- 0.324m, -0.003m, 0.400m] that is measured by the 3D Cad Tool, is called Pro-Engineer. The theoretical natural frequency of the system with the previous rigid foot is 5.5 (rad/s) when the gravity acceleration is 9.81 (m/s^2). So, the resonance frequency of the same system is a little bigger than the natural frequency. The method to find the natural frequency and total stiffness of the system is to make excitation at its ankle joint. The fast fourier transform shows the resonance frequency of the system. And using the curve fitting tool of MATLAB, we are obtained the total stiffness. In order to get the resonance frequency, random excitation is performed using frequency sweeps method. Using ZMP, we verify the performance of the proposed foot. The ZMP is calculated as shown below.

$$P_{Zx} = \frac{f_{Sx}p_{Zz} - P_{S2}}{f_{Sz}}, \quad P_{Zy} = \frac{f_{Sy}p_{Zz} - P_{S1}}{f_{Sz}} \tag{10}$$

where the set of force-torque sensor position, measured force and moment is $\{p_S, f_S, n_S\}$, $P_{S1} = f_{Sz}p_{Sy} - f_{Sy}p_{Sz} +$

n_{Sx}, $P_{S2} = f_{Sx}p_{Sz} - f_{Sz}p_{Sx} + n_{Sy}$ are substituted for equation (10).

$$p_{Zx} = \frac{f_{Sx}}{f_{Sz}}(p_{Zz} - p_{Sz}) + p_{Sx} - \frac{n_{Sy}}{f_{Sz}} \tag{11}$$
$$p_{Zy} = \frac{f_{Sy}}{f_{Sz}}(p_{Zz} - p_{Sz}) + p_{Sy} - \frac{n_{Sx}}{f_{Sz}}$$

where p_{Zz} is zero because of the definition of ZMP. And S p is a fixed value because of that is a sensor position with respect to the base frame. The comparison of the ZMP between the previous rigid foot and the proposed foot with only bush, the proposed foot with the guide equipment is just related to force-torque data $f_{Sx}-n_{Sy}$, $f_{Sy}-n_{Sx}$ about p_{Zx}, p_{Zy}.

4.3 Result of excitation experiment

The result of the experiment is shown as Table 1.

Table 1. Resonance frequency and stiffness

Properties \ Foots			Rigid foot	Proposed foot	Guide only	Bush only
Pitch joint	Resonance frequency (Hz)	first	7.23	5.87	4.94	4.82
		second	13.34	12.85	12.64	12.55
	Stiffness		-174.1	-152.63	-88.23	-85.89
Roll joint	Resonance frequency (Hz)	first	6.67	5.45	4.39	4.23
		second	13.34	12.88	12.61	12.60
	Stiffness		54.29	50.22	21.83	20.76

where the stiffness means the total stiffness which includes the landing leg. The stiffness unit is Nm/deg. In Table.1, the proposed foot without guide stopper is useless because that the difference between the foot with bush only and the foot without guide stopper is small about the resonance frequency and the stiffness.

The stiffness of the proposed foot is 87.67the pitch and roll joint with respect to the stiffness of the rigid foot respectively. On the contrary, the foot with bush only is 49.33the stiffness of the rigid foot respectively. This result presents that the stiffness of lateral direction of proposed foot is placed after the rigid foot and thats meant that using the proposed foot instead of the previous foot is an easy task. The result of resonance frequency shows the same conclusion.

Fig.12 shows results of ZMP variations about each foot. The proposed foot mechanism can reduce translational movement and induced force by bush. The proposed foot with only bush has the some quadruple of the ZMP variation compared with the previous rigid foot.

5. CONCLUSION

The most important function of the proposed foot mechanism is to absorb the shock of ground reaction force. And the ZMP variation is absent simultaneously. The shock absorbing performance is improved by adding the bush. And the lateral movement induced by the bush is reduced by the guide equipment. However, the proposed foot does not achieve the same effect about stiffness and resonance frequency that previous rigid foot makes. Fortunately, the Proposed foot's ZMP variaion that brings about instability of humaonid working is almost similar with the rigid foot. Therefore the proposed foot in this paper is expected to show fair performance in humanoid walking.

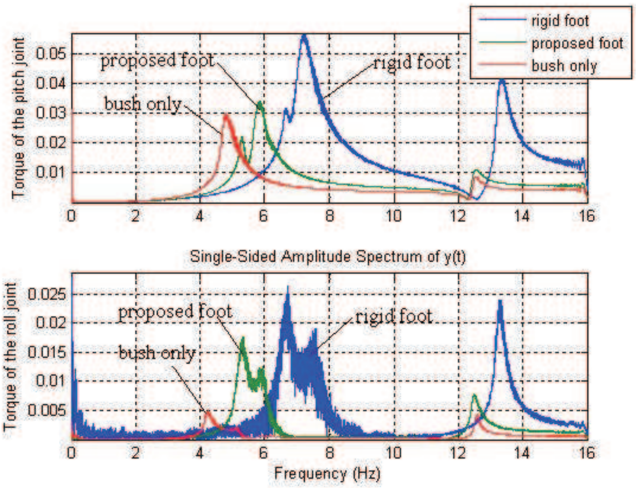

Fig. 11. Comparison between the resonance frequency of each foot about the pitch and the roll joint

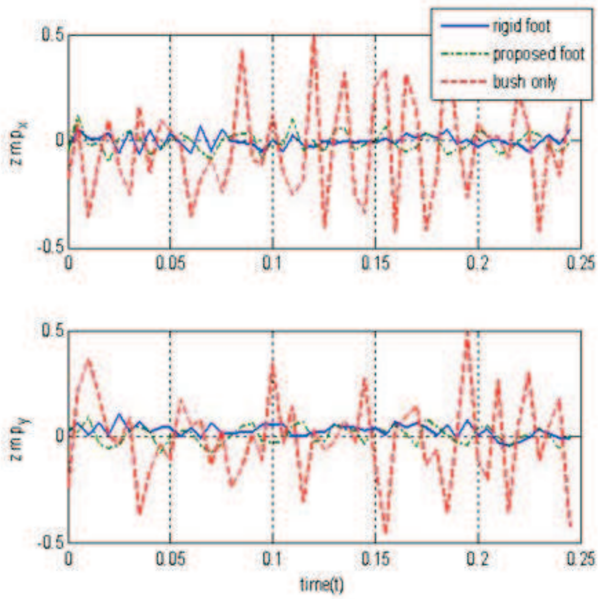

Fig. 12. Comparison of the ZMP between the each foot

ACKNOWLEDGEMENTS

This work was supported by IT R&D.

REFERENCES

B. J. You, Y. Choi, M. Jeong, D. Kim, Y. H. Oh, C. Kim, J. S. Cho, M. Park, and S. Oh. Network-based Humanoids 'MAHRU' and 'AHRA'. *Int. Conf. Ubiquitous Robots and Ambient Intelligence*, pages 376–379, 2005.

I. W. Park, J. Y. Kim, J. H. Oh. Mechanical Design of Humanoid Robot Platform KHR-3 (KAIST Humanoid Robot.3: HUBO). *Int. Conf. on Humanoid Robots*, 2005.

J. H. Kim, J. H. Oh. Walking Control of the Humanoid platform KHR-1 base on Torque Feedback Control. *Int. Conf. on Robotics and Automation*, volume 44, pages 623–628, 2004.

K. Hirai, M. Hirose, Y. Haikawa, T. Takenaka. The Development of Honda Humanoid Robot. *in Proc. IEEE Int. Conf. on Robotics and Automations*, pages 1321–1326, 1998.

L. Sciavicco and B. Siciliano. Modeling and control of robot manipulators. *McGraw-Hill, NewYork*, pages 21–129, 1996.

S. Kajita, K. Yokoi, M. Saigo, K. Tanie. Balancing a Humanoid Robot Using Backdrive Concerned Torque Control and Direct Angular Momentum Feedback. *Int. Conf. on Robotics and Automations*, pages 3376–3382, 2001.